WELDING RESEARCH

SUPPLEMENT TO THE *WELDING JOURNAL*, OCTOBER 2006
Sponsored by the American Welding Society and the Welding Research Council

Structural Stability of Dissimilar Weld between Two Cr-Mo-V Steels

Results are presented of an experimental study and modeling of the structural stability of 6Cr-Mo-V 8-3-2 and X12Cr-Mo-Nb 10-1 steels in a temperature interval from 600° to 900°C

BY R. FORET, B. ZLAMAL, AND J. SOPOUSEK

ABSTRACT. Heterogeneous weld joints of creep-resistant steels are used with increasing frequency in the construction of new or repair and reconstruction of existing power-generating and chemical industry facilities. These weld joints show structural instability during postweld heat treatment (PWHT) and in the course of subsequent operations. Carbon redistribution and subsequent sequence of changes in the structure lead to the formation of a carbon-depleted zone (CDZ) in low-alloy steel. On the contrary, a carbon-enriched zone (CEZ) appears in high-alloy steel, with the differences in chromium content having the greatest significance.

This paper presents the results of a study of structural changes in laboratory welds of 6Cr-Mo-V 8-3-2 (T25) and X12Cr-Mo-V-Nb 10-1 (P91) steels annealed at temperatures from 600° to 900°C (1112° to 1652°F). Carbon redistribution measurements by the EPMA method were complemented with detailed structural analyses aimed at the phase and chemical compositions of coexisting carbides and carbonitrides.

The results of experimental work were compared with thermodynamic and kinetic calculations using the *Thermo-Calc* and *DICTRA* software. A very good agreement between the calculations and the experiments was obtained, in particular for the phase composition of individual areas of the weld joints.

Introduction

An integral part of the development of creep-resistant steels with ferritic matrix is the study of the degradation processes occurring during their operation in power-generating and chemical plants, inclusive of the structural instability of both the steels themselves and their weld joints.

The term structural instability usually refers to the successive microstructural changes toward equilibrium state, when the Gibbs energy is minimal, and with creep-resistant steels, the metastable minority phases dissolve and the stable ones precipitate, and the density of dislocations and the size of grain boundary area (phase interface) decrease. An example of the effect of structural instability on the creep properties of some modified 9–12% Cr steels is their sigmoidal behavior (Ref. 1).

In view of the exhausted service life of a number of power-generating blocks (2×10^5 and more hours of operation) and with regard to the growing power demand, increased capital investment is expected in the area of constructing conventional power plants. It can be expected that in the construction of new power-generating blocks and in the reconstruction of existing blocks attention will focus on increasing their efficiency, which will entail continuous development of creep-resistant steels with a ferritic matrix (Refs. 2, 3).

Both nuclear and conventional power plants are complex systems in which it is practically impossible to rule out welding different kinds of creep-resistant steel. A redistribution of interstitials (C, N, and H) in dissimilar weld joints of austenite/ferrite type and ferrite/ferrite type can be observed within welding and subsequent PWHT or in the course of the welds exploitation at elevated temperatures. The interstitials redistribution can cause the formation of carbon-depleted zones (CDZ) in low-alloy steels, and on the contrary, the formation of carbon-enriched zones (CEZ) in high-alloy steels, both of them in a close vicinity to the fusion zone. The appearance of the above zones is determined by the type of steels being welded, by the conditions of PWHT, and by the exploitation itself. The structure of the carbon-depleted zone is usually formed by ferritic grains without any apparent carbide precipitate (Refs. 4–6), in which the localization of plastic deformation may occur and the state of triaxial stress appears.

In Ref. 7 it is stated that three principal cracking mechanisms affecting Cr-Mo-V welds are reheat cracking, Type IV cracking, and Type IIIa cracking. In Ref. 4, a detailed description is given of the differences between reheat cracking and Type IIIa cracking, adding that Type IIIa cracking is due to the above carbon migration. Helander, Andersson, and Oskarsson (Ref. 8) observed that the influence of the CDZ on the creep strength of the weld has been the subject of some controversy over the years. Some authors suggest that it has a significant influence on the mechanical properties (Ref. 9), while others considered the influence negligible (Ref. 10). Also ambiguous are the results of the effect of the time of operation (creep tests) on the occurrence of Type IIIa failure. The behavior of a weld of the type of 1%Cr-Mo-V/12%Cr-Mo-V studied in (Ref. 9) is determined in short-time creep testing by heterogeneous microstructural features. In the case of welds of 2.25%Cr-Mo/12%Cr-Mo-W-V steels,

R. FORET (foret@fme.vutbr.cz) *and B. ZLAMAL are with Brno University of Technology, Faculty of Mechanical Engineering, Department of Materials Science and Engineering, Brno, Czech Republic. J. SOPOUSEK is with Masaryk University Brno, Faculty of Science, Department of Theoretical and Physical Chemistry, Brno, Czech Republic.*

KEYWORDS

Creep-Resistant Steel
Weld Joints
Structural Analyses
Thermodynamic Modeling
Kinetic Modeling

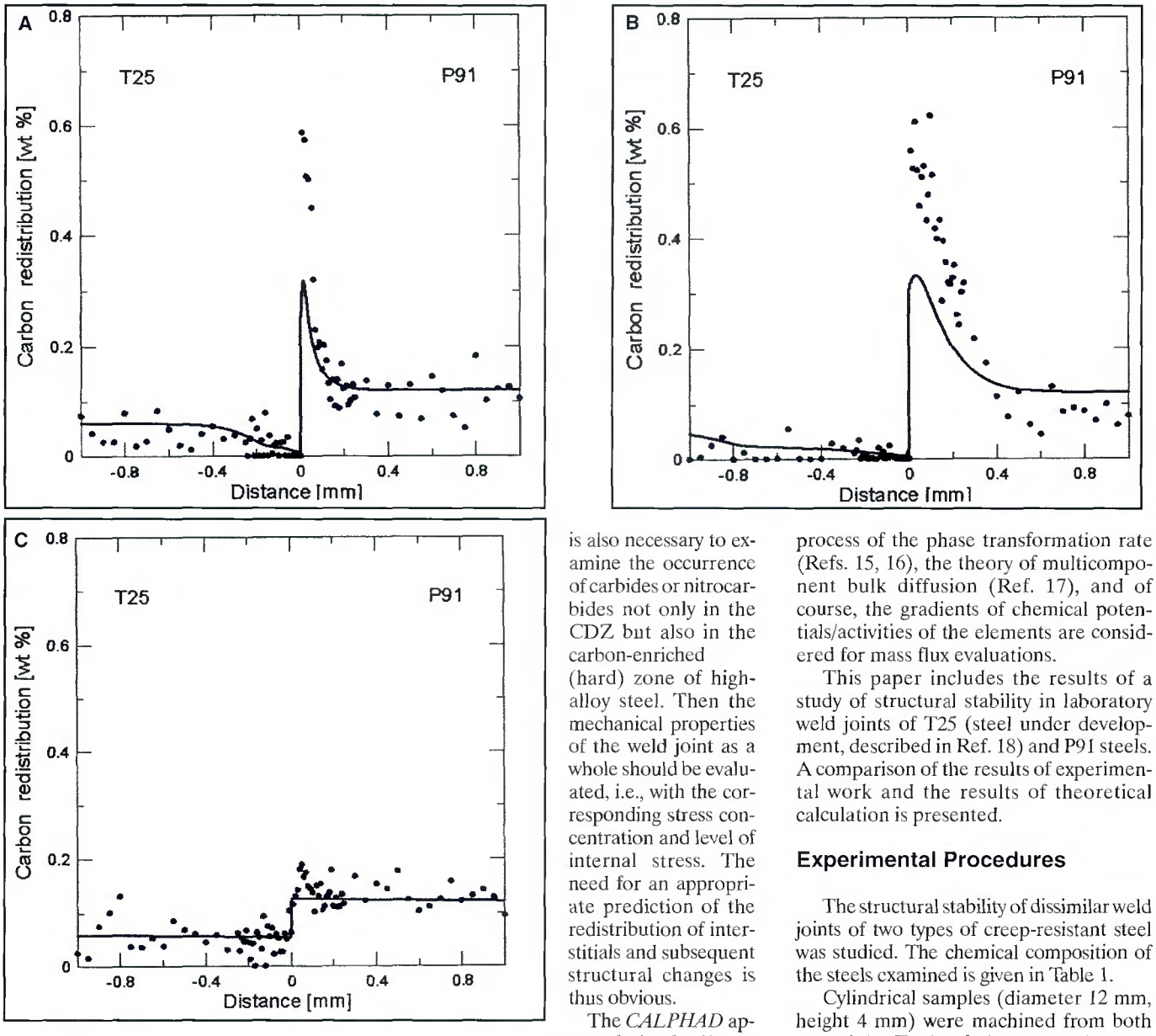

Fig. 1 — Comparison of simulated and measured redistribution of carbon in the weld joint T25/P91 annealed at different conditions (simulation measurement by EPMA method). A — 600°C/240 h; B — 700°C/56 h; C — 900°C/18 h — (simulation, ...measument by EPMA method).

Type IIIa failure was observed only after longer creep stress times (Ref. 8). Likewise, Albert et al. (Ref. 11) reported that the occurrence of CDZ and CEZ in heterogenous weld joints is of pronounced negative effect on their toughness at room temperature. As regards the creep characteristics, this effect is ambiguous in the case of type ferrite/ferrite welds, while in the case of type ferrite/austenite welds the degradation of these characteristics predominates.

The effect of CDZ on mechanical properties, inclusive of the creep characteristics, must be considered comprehensively. Besides the carbon depletion itself, assessed by the zone width and carbon concentration, it is also necessary to examine the occurrence of carbides or nitrocarbides not only in the CDZ but also in the carbon-enriched (hard) zone of high-alloy steel. Then the mechanical properties of the weld joint as a whole should be evaluated, i.e., with the corresponding stress concentration and level of internal stress. The need for an appropriate prediction of the redistribution of interstitials and subsequent structural changes is thus obvious.

The *CALPHAD* approach (Ref. 12) can be used for the solution of both local and global phase equilibrium problems concerning the base material and weld joints. The approach enables the calculation of chemical compositions of equilibrated phases at a given temperature as well as any of the phase diagram cross sections. Also important is the possibility to calculate the chemical potentials/activities of elements.

The *DICTRA* program (Ref. 13), which contains subroutines for the *CALPHAD* method, is used as a conductive tool to simulate processes in dissimilar welds. The benefits of using the *DICTRA* program are described in Ref. 14. This program embodies the assumption of local condition of phase equilibrium, the assumption that diffusion is the controlling process of the phase transformation rate (Refs. 15, 16), the theory of multicomponent bulk diffusion (Ref. 17), and of course, the gradients of chemical potentials/activities of the elements are considered for mass flux evaluations.

This paper includes the results of a study of structural stability in laboratory weld joints of T25 (steel under development, described in Ref. 18) and P91 steels. A comparison of the results of experimental work and the results of theoretical calculation is presented.

Experimental Procedures

The structural stability of dissimilar weld joints of two types of creep-resistant steel was studied. The chemical composition of the steels examined is given in Table 1.

Cylindrical samples (diameter 12 mm, height 4 mm) were machined from both materials. Each of these samples was ground and polished, and pairs were welded to form "sandwich-type" couples. The laboratory weld joints were prepared via AC heating to a temperature of 800°C (1472°F) within ~20 s, with subsequent heating to a temperature 1050°C (1922°F) within ~5 s. Welding was conducted in an atmosphere of argon under a thrust force of 200 N. These samples were sealed into evacuated quartz ampoules and annealed as shown in Table 2.

After annealing, the joints were cut perpendicularly to the weld interface. Analyses of microstructure were then carried out on these surfaces, with Vilella's reagent and 2% nital reagent being used to produce the structure.

The carbon motion across the welds was measured by means of wavelength dispersive X-ray analysis (WDX) in a Jeol JXA-8600 electron probe microanalyzer

Fig. 2 — Microstructure of the weld zone, steel T25 is located on upper part (SEM micrograph).

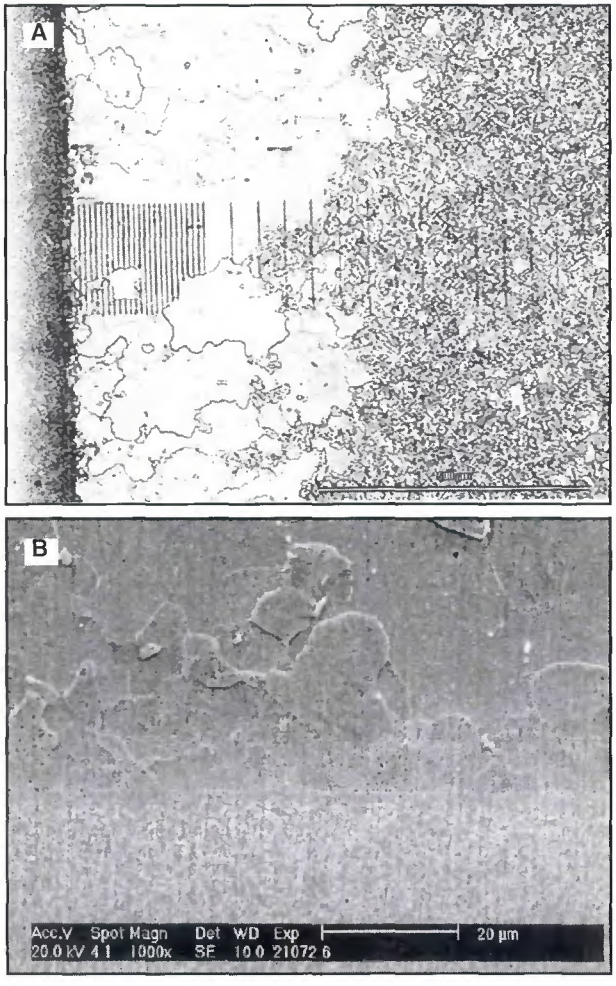

Fig. 3 — A — Microstructure of the CDZ and CEZ (annealed 700°C/56h) with contamination path from EPMA measurement (light microscopy); B — detail of the weld joint interface from Fig. 3A (SEM micrograph).

(EPMA). A transmission electron microscope Philips CM12 working in the scanning mode (STEM) equipped with energy dispersive X-ray (EDX) Phoenix analyzer, and selected area electron diffraction (SAED) were used to determine the characteristics of microstructure from carbon extraction replicas. A combination of diffraction data and chemical composition was used for phase identification, especially for the carbides.

Model calculations were conducted using the *Thermo-Calc* and the *DICTRA* software and utilizing the *STEEL* 16.tdb database (Ref. 19) and the Dif.tdb kinetics database (Ref. 20).

Experimental Results

The measured carbon concentration profiles across the weld interface are given in Fig. 1. As expected, carbon diffused from the T25 low-alloy steel into the P91 high-alloy steel. In view of the low carbon concentration of the two steels (in the CDZ in particular) and considering the scatter of the values measured, which is due to the occurrence of carbide phases, it was not possible to determine reliably the carbon content in the CDZ. The measurement of CDZ widths is also only approximate. The maximum carbon concentrations in the CEZ (C_{max}) are given in Table 2, together with estimates of CDZ and CEZ widths. If during annealing the matrices of the two steels are austenitic (a temperature of 900°C), the redistribution of carbon is little pronounced. If, however, the above matrices are ferritic, the redistribution of carbon is considerable, with the C_{max} concentration values in the interval 0.6–0.7 wt-% and in agreement with the values measured by Buchmayr et al. (Ref. 9). With increasing annealing temperature in the ferrite region, there is a tendency for the C_{max} values to grow while there is a considerable increase in the width of carbon-enriched zones, which means that the amount of redistributed carbon increases.

The microstructure of the weld interface depends on the annealing temperature and on the amount of redistributed carbon. At annealing temperatures of

Table 1 — Chemical Composition of Steels (wt-%)

Steel	C	Mn	Si	P	S	Cr	Mo	V	B	Al	N	Nb	Fe
T25	0.06	0.42	0.34	0.012	0.011	1.91	0.31	0.22	0.003	0.009	0.024	0.058	bal.
P91	0.12	0.38	0.44	0.010	0.003	9.96	0.89	0.22	—	0.010	0.069	0.070	bal.

Table 2 — Heat Treatment and Basic Characteristics of Carbon Redistribution

Sample No.	Annealing		Experimental Results			Results of Modeling			
	T[°C (°F)]	t(h)	C_{max} (wt-%)	width of CDZ and CEZ (mm)		C_{max} (wt-%)	C_{min} (wt-%)	width of CDZ and CEZ (mm)	
3	900 (1652)	18	0.19	—	0.55	0.125	0.055	1.2	1.0
6	700 (1292)	56	0.65	1.0	0.30	0.33	0.01	1.3	0.5
7	600 (1112)	240	0.60	0.4	0.20	0.31	0.01	0.7	0.3

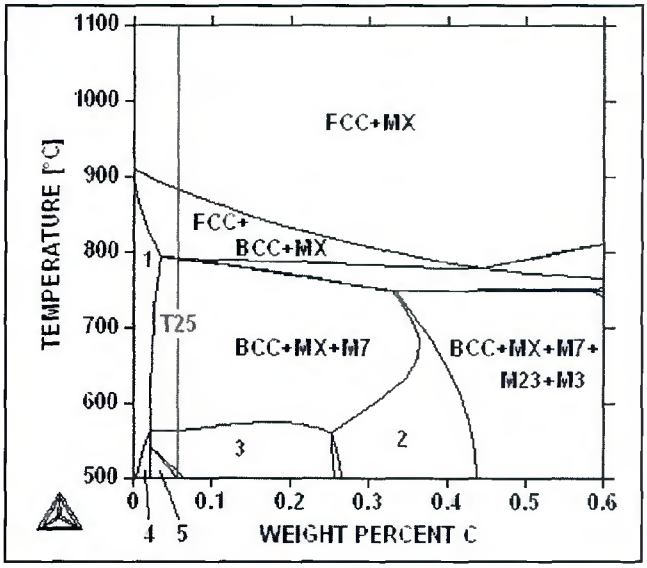

Fig. 4 — Phase diagram for base T25 steel. Red line represents carbon content. Phase fields: 1...BCC + MX, 2...BCC + MX + M23 + M7, 3...BCC + MX + M7+M6, 4...BCC + MX + M6, 5...BCC + MX + M23 + M6.

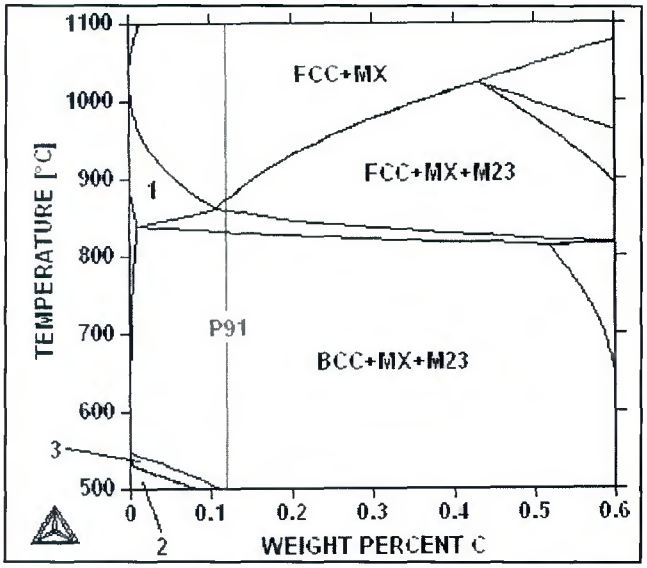

Fig. 5 — Phase diagram for base P91 steel. Red line represents carbon content. Phase fields: 1...BCC + FCC + MX, 2...BCC + MX + M6 + LAVES, 3...BCC + MX + M6 + M23.

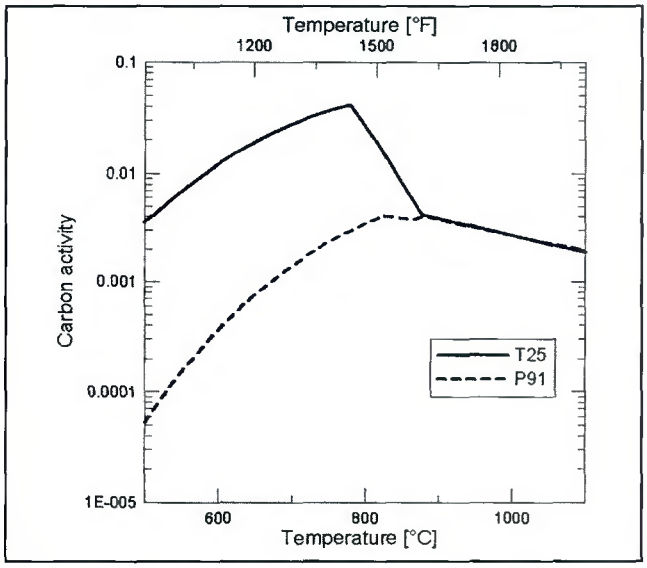

Fig. 6 — Temperature dependence of carbon activity in base T25 and P91 steels.

900°C (1652°F) and higher, when the matrix of the two steels is austenitic, subsequent cooling in air results in martensitic transformation of the P91 steel and predominantly bainitic transformation of the T25 steel. In these structures, carbon depletion and carbon enrichment are difficult to observe, as can be seen in Fig. 2.

A typical structure of the weld interface of a sample annealed at a temperature of 700°C (1292°F) can be seen in Fig. 3. The CDZ of the T25 steel is formed by ferritic grains of irregular shape (Fig. 3A), in which relatively coarse precipitates can be seen to occur — Fig. 3B. At an annealing temperature of 600°C (1112°F), the initial bainite morphology remains partly preserved in the CDZ. In comparison with the nonaffected region, a markedly increased density of carbides can be observed in the CEZ of the P91 steel — Fig. 3B.

Results of the analyses of minority phases in individual regions of the weld joints under study are given in Table 3. At a temperature of 900°C (1652°F) only phase MX (X = C,N) occurs in the T25 steel while $M_{23}C_6$ and MX could be observed in the P91 steel. At a temperature of 600°C (1112°F), M_7C_3 and MX are found in nonaffected T25 material; carbon depletion led to the dissolution of carbides M_7C_3. Thus only the MX phase occurs in the CDZ, which was also established for annealing temperatures of 500° and 700°C (932° and 1292°F). In the P91 steel at 600°C (1112°F), the minority phases are formed by $M_{23}C_6$ + MX + M_2X, and carbon enrichment does not alter the phase composition.

In the two steels an NbX primary phase occurs, not dissolved in the course of austenitization, in which the content of Nb ranges between 27 and 39 at.-%. This phase also contains 7–22 at.-% of V. The chemical composition of secondary MX phases varies considerably, which is probably related to the difficulty with which equilibrium states are achieved. The secondary MX phases could be divided into two groups. The phase denoted $MX^{(2)}$ is a nitride or a carbonitride with vanadium predominating (35–41 at.-%), and it also contains small amounts of Nb (4–7 at.-%) and Cr (1—10 at.-%). The composition obtained by calculation is almost identical. The composition of the metallic part of phase $MX^{(2)}$ does not depend on steel composition and annealing temperature. The phase denoted $MX^{(1)}$ occurs in the T25 steel and in comparison with $MX^{(2)}$, it has a lower content of V (27–30 at.-%) and a higher content of Nb (15–21 at.-%). Judging from the chemical composition, it is a transition type between NbX and $MX^{(2)}$. In this case simultaneous analyses of both particles or heterogeneous nucleation of MX particles on nondissolved primary NbX particles cannot be ruled out.

Equilibrium Predictions

The *CALPHAD* approach (Ref. 12) and the *STEEL* thermodynamic database (Ref. 19) were used for the solution of both local and global phase equilibrium problems concerning the base material (T25, P91), and weld joints of these steels. The phases that can be found in the system are different and the thermodynamic description is given in Ref. 20. A list of phases is given in Table 4, which also gives the abbreviations used for phases in this paper. The calculated stable phase diagram cross sections for the base T25 and P91 steels, whose composition is given in Table 1, are given in Figs. 4, 5.

It is evident from the values given in Table 3 that the experimental results tally with the thermodynamic calculations except for the P91 base material, where $M_{23}C_6$ + MX should have occurred by calculation.

Table 3 — Coexisting Phases and Their Chemical Composition (at.-%)

		Experimental[a]					Calculation							
	Phase	V	Cr	Fe	Nb	Mo	Phase	V	Cr	Fe	Nb	Mo	C	N
900°C (1650°F)														
BMT	$MX^{(2)}$	38.5	2.4	0.9	5.4	3.0	$MX^{(2)}$	40.2	1.0	0.0	11.4	0.2	33.0	14.4
	$MX^{(1)}$	27.1	1.2	1.1	17.7	3.0								
	NbX	16.1	0.4	0.4	32.1	1.1								
CDZ	$MX^{(2)}$	40.8	2.2	0.5	4.8	1.8	$MX^{(2)}$	39.6	0.5	0.0	12.5	0.2	0.5	46.9
	$MX^{(1)}$	27.2	0.7	0.3	21.1	0.7								
	NbX	17.3	0.6	0.5	30.6	1.1								
CEZ	$M_{23}C_6$	1.7	47.5	25.5	0.6	4.0	$M_{23}C_6$	1.1	47.5	27.7	0.0	2.8	20.7	0.0
	$MX^{(2)}$	35.1	7.5	0.7	6.2	0.7	$MX^{(2)}$	35.3	8.9	0.0	7.6	0.1	7.3	40.1
	NbX	7.0	1.9	1.0	38.8	1.4								
MBP	$M_{23}C_6$	1.3	47.3	26.3	0.5	4.0								
	$MX^{(2)}$	35.9	6.1	0.3	7.3	0.6	$MX^{(2)}$	36.1	8.2	0.0	7.6	0.1	6.5	41.6
	NbX	7.5	2.6	0.9	37.9	1.3								
600°C (1100°F)														
BMT	M_7C_3	4.1	35.3	28.9	0.6	1.1	M_7C_3	1.9	54.7	10.7	0.0	0.8	30.0	0.0
	$MX^{(2)}$	33.6	6.0	1.5	4.1	5.0	$MX^{(2)}$	44.9	1.9	2.9	4.9	0.0	26.6	21.6
	$MX^{(1)}$	29.7	2.4	0.6	15.0	2.4	$MX^{(1)}$	26.8	0.1	0.0	20.4	3.7	46.4	1.8
	NbX	16.6	0.7	0.4	31.2	1.2								
CDZ	$MX^{(2)}$	39.9	3.2	0.6	3.7	2.7	$MX^{(2)}$	39.3	0.5	0.0	13.7	0.0	5.9	40.6
	NbX	21.6	0.7	0.3	26.6	1.0								
CEZ	$M_{23}C_6$	1.0	52.8	20.8	0.6	4.1	$M_{23}C_6$	0.3	56.5	18.8	0.0	3.3	20.7	0.0
	$MX^{(2)}$	34.9	10.2	0.65	3.6	0.6	$MX^{(2)}$	35.9	7.7	0.0	7.2	0.0	2.1	47.2
	M^2X	9.6	54.3	1.1	0.4	1.3								
BMP	$M_{23}C_6$	1.1	51.8	21.7	0.6	4.1	$M_{23}C_6$	0.4	62.8	12.7	0.0	3.1	20.7	0.0
	$MX^{(2)}$	35.9	9.8	0.6	3.2	0.6	$MX^{(2)}$	38.1	5.8	0.0	7.3	0.0	1.1	47.7
	NbX	7.4	2.4	1.0	38.0	1.3								
	M_2X	9.3	53.1	1.1	0.7	2.5								

(a) Chemical composition of metallic part, BMT — base material, steel T25; BMP — base material, steel P91.

Table 4 — Phase Abbreviations Used in the Figures

Phase	Austenite	Ferrite	$M_{23}C_6$	M_7C_3	M_3C	M_6C	Laves Phase	M_2X Carbonitride	MX Carbonitride
Abr.	FCC	BCC	M23	M7	M3	M6	LAVES	M2	MX

In the case of experiments, an analysis of nonequilibrium state is probably involved here since M_2X is usually substituted by the MX phase only after longer periods of annealing. It follows from Table 3 that, according to the calculation, the MX phase in the two steels is generally a carbonitride, with the ratio of C content to N content depending on the type of steel and on the preceding thermal history. In the T25 steel we are concerned with carbonitrides with predominant proportion of C, the content of which varies from 27 to 46 at.-% while in the P91 steel almost pure nitrides are involved, which is confirmed by literature searches conducted in Ref. 21. For annealing at a temperature of 900°C (1652°F) the calculated composition and the measured composition of the occurring minority phases are in principle identical. For a temperature of 600°C (1112°F), the two compositions are either the same or the calculated composition exhibits a higher content of elements of higher affinity to carbon or nitrogen (higher content of C at the expense of Fe in the case of carbides $M_{23}C_6$ and M_7C_3, and a higher proportion of V at the expense of Cr and Mo in the MX carbonitrides). The above differences are again related to the insufficient annealing times for reaching equilibrium states at lower annealing temperatures.

An important result of phase equilibrium calculations is the evaluation of the activities of individual elements in the steels with respect to standard element reference (SGTE) (Ref. 22). The activity difference of the given element in two different materials can be used as a first approximation for weld joint stability assessment (Ref. 23) because each element diffuses to a place with its lower activity and this diffusion flux is roughly proportional to the absolute value of the activity difference. In the case of the microstructure evolution of dissimilar welds of steels, interstitial elements (such as carbon, nitrogen, and hydrogen) are of utmost importance because they diffuse more quickly than substitution elements. Thus the diffusion of the metal elements can be neglected. Along with the carbon redistribution, the redistribution of Fe, Cr, and Mo was also measured. These analyses confirmed that width of the fusion zone and the diffusion zone of substitution elements does not exceed the value 5 μm and can thus be neglected.

The temperature dependence of the carbon activity for the examined steels is given in Fig. 6. In spite of the higher carbon content (0.12 wt-%) in the P91 steel and the lower carbon content (0.06 wt-%) in the

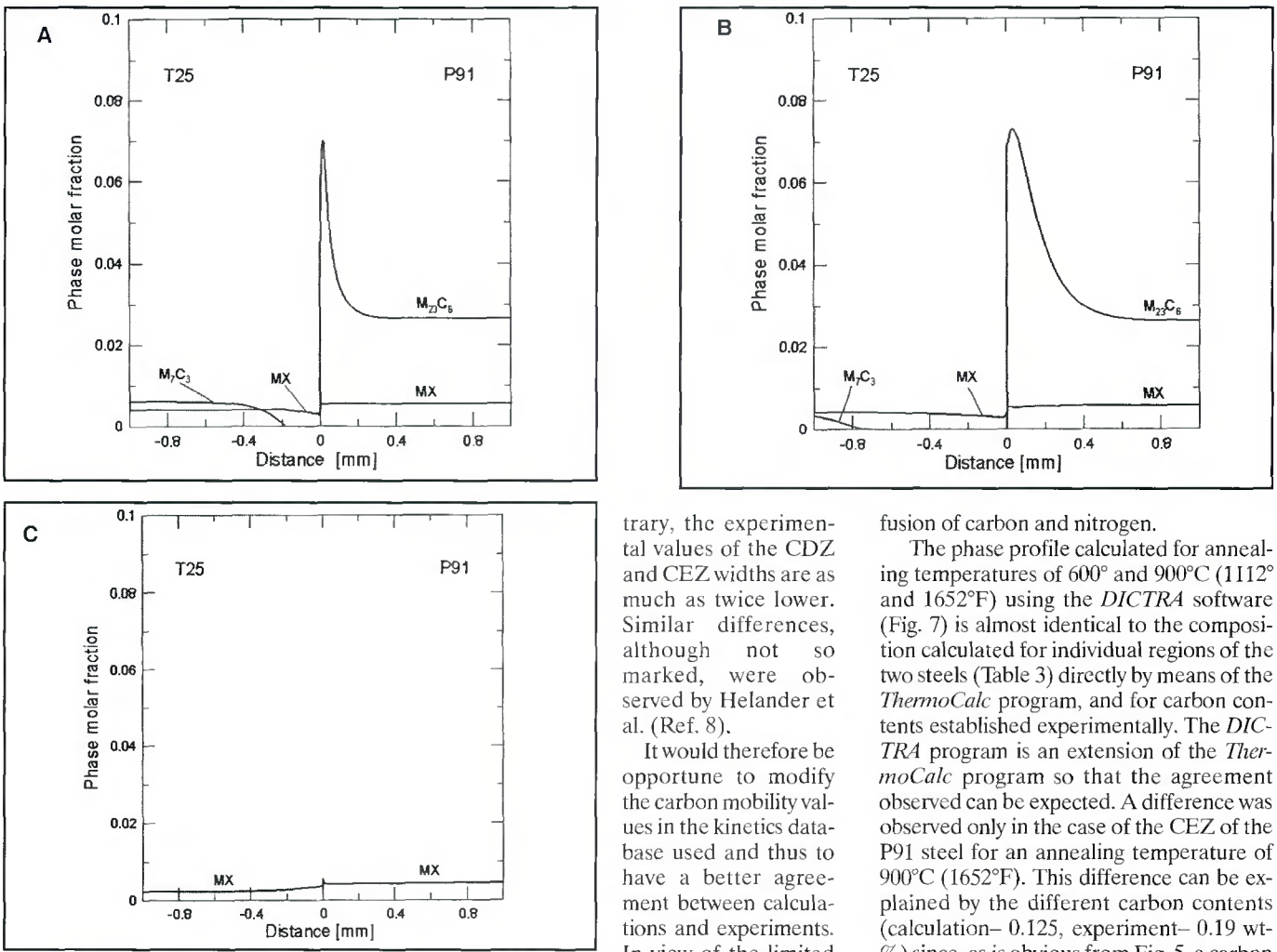

Fig. 7 — Phase profiles in the weld joint T25/P91 annealed at different conditions. A — 600°C/240 h; B — 700°C/56 h; C — 900°C/18 h.

T25 steel, Fig. 6 predicts that the carbon will diffuse from T25 to P91 at low temperatures, ranging from 500° to 870°C (i.e., carbon up-hill diffusion). At temperatures higher than 870°C (1598°F), when the matrices of the two steels are completely austenitic, the differences in activities are substantially smaller; consequently, the carbon redistribution is also markedly lower, as was experimentally confirmed — Fig. 1.

Discussion

The weld joint of the two advanced creep-resistant steels is structurally unstable due to the carbon redistribution, which continues to proceed even at a temperature of 800°C (1472°F). The dependence relations given in Fig. 1 confirm the conclusions resulting from the temperature dependence of carbon activity in the matrices of the two steels and are in agreement with experimental results. The C_{max} values measured are approximately twice the calculated value; on the contrary, the experimental values of the CDZ and CEZ widths are as much as twice lower. Similar differences, although not so marked, were observed by Helander et al. (Ref. 8).

It would therefore be opportune to modify the carbon mobility values in the kinetics database used and thus to have a better agreement between calculations and experiments. In view of the limited extent of experimental work and in view of the difficulties involved when measuring by the EPMA method the low carbon concentrations in multiphase systems, this change would at present be only formal. Another possible cause of the disagreement observed may be the assumption of phase equilibrium in every computation cell, which is not fulfilled for low temperatures and short annealing times.

The accuracy of the thermodynamic and kinetic calculations used is currently given primarily by the accuracy of the databases used. The above good agreement between the calculated and the experimentally verified phase composition (inclusive of the chemical composition of individual phases) and the semiquantitative agreement in carbon distribution across the weld interface prove the consistency of the databases that are used and the building of which should be continued. Advanced creep-resistant steels contain, among other things, nitrogen, which due to its high diffusion mobility and low solubility in ferrite behaves analogously to carbon, and in the case of steels, attention must be given to simultaneous diffusion of carbon and nitrogen.

The phase profile calculated for annealing temperatures of 600° and 900°C (1112° and 1652°F) using the *DICTRA* software (Fig. 7) is almost identical to the composition calculated for individual regions of the two steels (Table 3) directly by means of the *ThermoCalc* program, and for carbon contents established experimentally. The *DICTRA* program is an extension of the *ThermoCalc* program so that the agreement observed can be expected. A difference was observed only in the case of the CEZ of the P91 steel for an annealing temperature of 900°C (1652°F). This difference can be explained by the different carbon contents (calculation– 0.125, experiment– 0.19 wt-%) since, as is obvious from Fig. 5, a carbon concentration of 0.125 wt-% (calculated) relates to austenite and MX, while at a carbon concentration of 0.19 wt–%, it is austenite + $M_{23}C_6$ + MX that occur.

The question arises whether it is purposeful to continue building the two databases, and possibly, make the model used more specific from the viewpoint of practical applications. From this viewpoint the calculation of the CDZ width is of primary importance by reason of

- A direct measurement of the CDZ width by the EPMA method is costly, mostly impossible, and inaccurate (problems of the detectability of low C contents and in multiphase systems);
- the CDZ width might correlate with the critical crack length from the viewpoint of brittle, fatigue, and creep fractures.

In real heterogeneous weld joints of creep-resistant steels there will be at least two fusion zones, namely between the base metals and the filler metal whose composition will be between the compositions of both base metals so that the carbon activity gradients in individual matrices will be lower than in the joint types under evaluation. It also needs to be con-

sidered that both dissolution of minority phases in low-alloy steel and, on the contrary, precipitation of carbides and nitrides in high-alloy steel, result in solid solutions being enriched with and depleted of carbide- and nitride-forming elements, which leads to the difference in carbon activities being reduced on either side of the weld joint. With increasing annealing time (exploitation) the redistribution of carbon and nitrogen will thus be less intensive.

The appearance of the CDZ and CEZ in heterogeneous weld joints of creep-resistant steels operated at elevated temperatures is a regular process that can even lead to the appearance of Type IIIa cracking. The possible methods of suppressing the occurrence and development of this structural instability are as follows:

- use a diffusion barrier, e.g. a nickel alloy;
- minimize the PWHT temperature and time;
- choose the chemical composition of filler metals such that the differences in carbon activities are distributed uniformly among individual joint welds.

Thermodynamic calculations have shown that in the steels under study the carbon activity is most affected by the chromium content. The alloying base of both the base metals and the filler metals should be chosen also with respect to the thermodynamic stability of individual phases such that either the nondissolved phases remain in the CDZ or they dissolve for as long as possible. The knowledge obtained to date shows that nitrides or carbonitrides of V and Nb are considerably more stable than carbide phases in low-alloy Cr-Mo steels of the type 2.25Cr-1Mo.

Conclusions

The structural analyses conducted together with thermodynamic and kinetic model calculations have confirmed that heterogeneous weld joints of creep-resistant steels are usually structurally unstable. This instability is in essence due to the different carbon activities in individual base materials of the weld joint. In the given case, carbon diffused by the so-called uphill diffusion from the T25 low-alloy steel (6Cr-Mo-V 8-3-2) into the P91 high-alloy steel (X12Cr-Mo-V-Nb10-1). The redistribution of carbon, which is substantially larger in the ferritic matrix than in the austenitic matrix, led to the appearance of CDZ in the T25 steel and CEZ in the P91 steel.

In the CDZ of steel T25, there was a complete dissolution of carbides M_7C_3 and partial dissolution of phase MX. No complete dissolution of the MX phase was observed in the T25 steel, not even at a temperature of 900°C (1652°F), but in spite of this, the recrystallization of ferrite was observed in the CDZ at temperatures of 700°C (1292°F) and higher. In the CEZ of steel P91 further precipitation of carbides $M_{23}C_6$ could be observed, provided the matrix of this steel was at least partially ferritic.

The experimentally established chemical and phase compositions of annealed weld joints were confirmed by thermodynamic and kinetic calculations using the *Thermo-Calc* and the *DICTRA* software, with very good agreement being obtained for the phase composition. The calculated and the experimentally established carbon concentration profiles exhibit sufficient agreement. The observed lack of agreement was connected with the analyses of nonequilibrium structural states and with neglecting a probably simultaneous diffusion of carbon and nitrogen.

Acknowledgments

The present work was supported by the Grant Agency of the Czech Republic under project No. 16/03/0636, and by the Ministry of Education, Youth, and Sports, Project No. MSM0021630508.

References

1. Strang, A., and Vodarek, V. 1998. Micro structural degradation of martensitic 12%Cr power plant steel during prolonged high temperature creep exposure. *Proc. of the 6th Liege Conference Materials for Advanced Power Engineering*, eds. J. Lecomte-Beckers et al., p. 601. Jülich: Forschungszentrum.

2. Masuyama, F. 2002. Trends in power engineering in Japan and requirements for improved materials and components. *Proc. of the 7th Liège Conference Materials for Advanced Power Engineering*, eds. J. Lecomte-Beckers et al. pp. 1767–1782. Jülich Forschungszentrum.

3. Mayer, K. H., et al. 2002. Development step soft new steels for advanced steam power plants. *Proc. of the 7th Liège Conference Materials for Advanced Power Engineering*, eds. J. Lecomte-Beckers et al. pp. 1385–1397. Jülich Forschungszentrum.

4. Brett, S. J. 2004. Type III cracking in 1/2CrMoV steam pipe work systems. *Science and Technology of Welding and Joining* 9(1): 41-s to 45-s.

5. Foret, R., et al. 2001. Structural stability of dissimilar weld joints of steel P91. *Science and Technology of Welding and Joining*, 6(6): 405-s to 411-s.

6. Sudha, C., et al. 2002. Systematic study of formation of soft and hard zones in dissimilar weldments of Cr-Mo steels. *Journal of Nuclear Materials* 302(4): 193-s to 205-s.

7. Bret, S. J. 1998. In-service cracking mechanism affecting 2CrMo welds in1/2CrMoV steam pipe work system. *Proc. of Int. Conf. Integrity of High-Temperature Welds*. pp. 3–14. Professional Engineering Publishing Ltd., London.

8. Helander, T., Andersson, C. M., and Oskarsson, M. 2000. Structural changes in 12-2.25 weldments — an experimental and theoretical approach. *Materials at High Temperatures* 17(3): 389-s to 396-s.

9. Buchmayr, B., et al. 1990. Experimental and numerical investigations of the creep behavior of the dissimilar weldment GS-17 CrMoV 5 11 and X 20 CrMoV 12 1. *Steel Research* 61(6): 268-s to 273-s.

10. Roberts, D. 1., Ryder, R., and Viswanathan, R. 1985. Performance of dissimilar welds in service. *Journal of Pressure Vessel Technology* 107(3): 247-s to 254-s.

11. Albert, S. K., et al. 1997. Soft zone formation in dissimilar welds between two Cr-Mo steels. *Welding Journal* 76 (3): 135-s to 142-s.

12. Saunders, N., and Miodovnik, A. P. 1998. *CALPHAD* (Calculation of Phase Diagram — A Comprehensive Guide). Amsterdam, Elsevier Science Publishing.

13. Anderson, J. O., et al. 2002. *Thermo-Calc* and *DICTRA*, computational tools for materials science. *CALPHAD*. 26: 273-s to 312-s.

14. Borgenstam, A., et al. 2000. *DICTRA*, a tool for simulation of diffusional transformations in alloys. *Journal of Phase Equilibria* 21(3): 269-s to 280-s.

15. Kirkaldy, J. S., and Young, D. J. 1985. *Diffusion in the Condensed State*, London, The Institute of Metals.

16. Engstram, A., Haglund, L., and Ägren, J. 1994. Computer simulation of diffusion in multiphase system. *Metallurgical and Materials Transactions A*. 25A(2): 1127-s to 1134-s.

17. Andersson, J. O., et al. 1990. Computer simulation of multicomponent diffusional transformations in steel. *Proc. Fundamentals and Applications of Ternary Diffusion*, ed. G. R. Purdy, pp. 153–163. Pergamon Press, New York.

18. Foldyna, V., et al. 2002. Microstructure and properties of modified 3%Cr steels. *Proc. of the 7th Liège Conference Materials for Advanced Power Engineering*. Eds. J. Lecomte-Beckers et al., pp. 1477–1486. Jülich Forschungszentrum.

19. Kroupa, A., et al. 2001. Phase diagram in the iron-rich corner of the Fe-Cr-Mo-V-C system below 1000 K. *Journal of Phase Equilibria* 22(3) :312-s to 323-s.

20. Sopousek, J., Jan, V., and Foret, R. 2004. Simulation of dissimilar weld joints of steel P91. *Science and Technology of Welding and Joining* 9(t): 59-s to 63-s.

21. Kubon, Z., Foldyna, V., and Vodarek, V. 1998. Optimized chemical composition of 9-12%Cr steels with respect to maximum creep resistance. *Proc.of the 6th Liege Conference Materials for Advanced Power Engineering*, eds. J. Lecomte-Beckers et al., pp. 311–325, Jülich: Forschungszentrum.

22. Dinsdale, A. T. 1991. SGTE data for pure elements. *CALPHAD* 15(4): 317-s to 425-s.

23. Jan, V., Sopousek, J., and Foret, R. 2004. Weld joint simulation of heat-resistant steels. *Archives of Metallurgy and Materials* 49(3): 469-s to 480-s.